A Molecular Dynamics Simulation of the Transport Properties of Molten (La$_{1/3}$, K)Cl

Masahiko Matsumiya and Koichi Seo

Department of Chemical Science and Engineering, Miyakonojo National College of Technology, 473-1, Yoshio, Miyakonojo, Miyazaki, 885-8567, Japan

Reprint requests to Prof. M. M.; Fax: +81-986-47-1231;
E-mail: mmatsumi@cc.miyakonojo-nct.ac.jp

Molecular dynamics simulations of molten (La$_{1/3}$, K)Cl at 1123 K have been performed in order to investigate the correlation between simulated dynamical properties such as the self-exchange velocity (v), the self-diffusion coefficient (D) and the electrical conductivity (κ) and the corresponding experimental values. The simulated results revealed that v and D of potassium decrease with increasing mole fraction of lanthanum, as expected from the experimental internal cation mobilities, b. The decrease of $b_{\rm K}$, $v_{\rm K}$ and $D_{\rm K}$ is ascribed to the tranquilization effect by La^{3+}, which strongly interacts with Cl$^-$. In contrast, $b_{\rm La}$, $v_{\rm La}$, and $D_{\rm La}$ increase with increasing concentration of La^{3+}. The distorted linkage of the network structure of [LaCl$_6$]$^{3-}$ units was disconnected with increasing the concentration of the alkali chloride. This might be attributed to the stronger association of La^{3+} with Cl$^-$ due to the enhanced charge asymmetry of the two cations neighboring Cl$^-$. The sequence of the calculated v's, D's, and κ's is consistent with those of the referred experimental results.

Key words: Internal Mobility; Molten Salts; Molecular Dynamics Simulation; Self-exchange Velocity.

1. Introduction

Besides the elecrowinning process using liquid metallic cathodes [1, 2], countercurrent electromigration [3, 4] has shown a significant possibility to recover rare earth (RE) elements, *e.g.* La^{3+} [5], Dy^{3+} [6], and Nd^{3+} [7] in a chloride bath. We have also estimated the limitation of the enrichment degree in alkali chloride and fluoride ternary [8, 9] and quaternary [10] melts by molecular dynamics (MD) simulation. Recently, we have demonstrated that the orders of self-exchange velocities (SEVs) obtained from MD simulation agree well with the experimental internal mobilities in molten DyCl$_3$-KCl [11] and NdCl$_3$-KCl [12]. In the present paper we examine the relationship between the computed and experimental transport properties of molten LaCl$_3$-KCl.

2. The Molecular Dynamics (MD) Simulation

The MD simulation proposed by Nose [13] with the 7 points predictor-corrector method was carried out using periodic boundaries in order to obtain a canoni-

cal ensemble. The Born-Mayer-Huggins pair potential, excluding the dipole-quadrupole term for LaCl$_3$-KCl mixtures, was employed in this simulation:

$$\Phi_{ij} = \frac{z_i z_j e^2}{r} + A_{ij} b \exp[(\sigma_i + \sigma_j - r)/\rho] - \frac{c_{ij}}{r^6}, \ (1)$$

where z and σ are the electric charge number and size parameter of the ion, A_{ij} is the Pauling factor between the ions i and j, and ρ is the softness parameter. A_{ij} is defined as

$$A_{ij} = \left(1 + \frac{z_i}{n_i} + \frac{z_j}{n_j}\right). \tag{2}$$

The Coulomb interaction between two ions was evaluated by the Ewald method [14]. The potential parameters of K$^+$ and Cl$^-$ given by Tosi and Fumi [15] were employed. The parameter c_{ij} was estimated from the ionic polarizability [16]. The side length of the periodic cell corresponded to the available density [17]. The corresponding parameters for the mixture were determined by the combination rule of Larsen *et al.* [18]. At the beginning, the cell in which the ions were

Table 1. Characteristic values of the $g_{ij}(r)$'s for cation-anion and anion-anion pairs in molten (La$_{1/3}$, K)Cl at 1123 K.

System (La : K)	Ion pair	R_1 /nm	R_M /nm	g (R_M)	R_2 /nm	R_m /nm	n_{eq} $(R_2 - R_m)$
(0.0:100.0)	K-Cl	0.260	0.295	3.71	0.369	0.472	3.90 − 5.46
(34.6:65.4)	K-Cl	0.266	0.299	2.51	0.371	0.463	3.99 − 6.37
(41.3:58.7)	K-Cl	0.264	0.300	2.40	0.372	0.453	4.17 − 6.34
(55.1:44.9)	K-Cl	0.267	0.302	2.21	0.374	0.452	4.70 − 7.27
(68.5:31.5)	K-Cl	0.270	0.303	2.02	0.378	0.465	4.88 − 8.21
(79.1:20.9)	K-Cl	0.270	0.304	1.91	0.376	0.461	5.08 − 8.37
(34.6:65.4)	La-Cl	0.255	0.282	8.77	0.334	0.413	6.45 − 7.21
(41.3:58.7)	La-Cl	0.251	0.279	8.34	0.332	0.414	6.39 − 7.13
(55.1:44.9)	La-Cl	0.253	0.281	6.88	0.332	0.413	6.55 − 7.59
(68.5:31.5)	La-Cl	0.251	0.279	6.46	0.330	0.409	6.42 − 7.79
(79.1:20.9)	La-Cl	0.251	0.277	5.98	0.328	0.405	6.36 − 7.63
(100.0:0.0)	La-Cl	0.248	0.276	5.50	0.324	0.403	6.18 − 7.54

R_1 and R_2 are the distances where $g_{ij}(r)$ crosses unity for the first and second time, respectively. R_M and R_m are the distances at the first maximum and minimum, respectively. $n_{eq}(R_2 - R_m)$ is the partial equivalent coordination number within $R_2 - R_m$ of a cation, which is equal to the coordination number of Cl$^-$ around the cation.

arranged in crystalline structure was annealed with the constant temperature method postulated by Woodcock [19]. After completion of the constant temperature by running several thousand steps, these were converted to constant energy runs. From the runs during more than 10^4 time steps, using Verlet's Algorithm by isothermal-choric (NVT) MD simulations after attainment of equilibrium, the structural and the dynamical properties were obtained. The self-diffusion coefficient was estimated from the mean square displacement, and the electrical conductivity was calculated by the Kubo formula [20] using 10^6 MD steps data.

3. Results and Discussion

The pair correlation functions $g(r)$ and the running coordination numbers $n(r)$ for increasing the mole fraction of La in this binary system are represented in Figure 1. Comparison of the pair correlation functions of pure LaCl$_3$ and KCl with those of the binary mixtures (La$_{1/3}$, K)Cl for various compositions, the position R_M of the first peak of g_{La-Cl} remains much the same. The nearest La-Cl and K-Cl distances for molten LaCl$_3$-KCl and some characteristic parameters are tabulated in Table 1 together with those of the pure melts.

As for the pure LaCl$_3$ melt, the ratio of $r_{Cl-Cl} = 0.347$ nm to $r_{La-Cl} = 0.275$ nm in the calculated pair correlation functions is roughly equal to $\sqrt{2}$ as calculated from the geometry of the octahedron. The number of Cl$^-$ ions around the La^{3+} ion is about 6. Thus it has been believed that the local structure of the trichloride
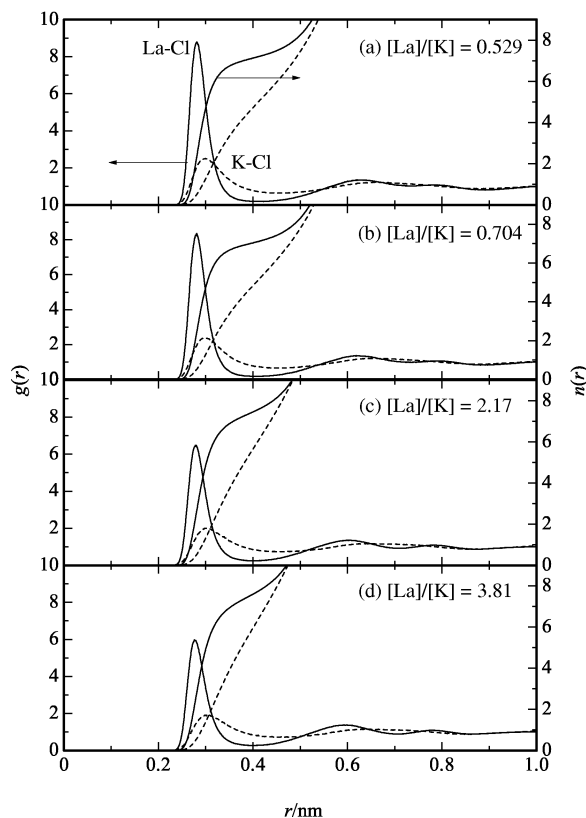

Fig. 1. Pair correlation functions $g(r)$ and running coordination numbers $n(r)$ of molten (La$_{1/3}$, K)Cl for four compositions; $g_{La-Cl}(r)$ and $n_{La-Cl}(r)$, solid lines; $g_{K-Cl}(r)$ and $n_{K-Cl}(r)$, broken lines.

melts has simply 6-fold the octahedral coordination [LaCl$_6$]$^{3-}$, because the vibration modes corresponding to the 6-fold octahedral coordination were observed for some rare earth trichloride melts in Raman spectroscopic studies [21, 22]. Moreover, the network structure of [LaCl$_3$]$^{6-}$ units could be considered as a distorted corner-sharings of 6-fold complex ions according to the correlation, $r_{Cl-Cl} < r_{La-La} < 2 \times r_{Cl-Cl}$. Recently, the XAFS diffraction study [23] of pure LaCl$_3$ melts also proposed that even in the pure melts the octahedral unit exists, which is connected to other units by distorted corner-sharing.

The nearest La-Cl distance is almost constant in the binary mixtures. The variation of the Cl$^-$ coordination number around the cations is shown in Figure 2. Around the La^{3+} ion it is nearly constant and is about six, which means that the octahedral structure is kept in the mixtures. Around the K$^+$ ion, however, it increases from 4 in pure KCl to 5 in 79.2% LaCl$_3$-KCl melt. As
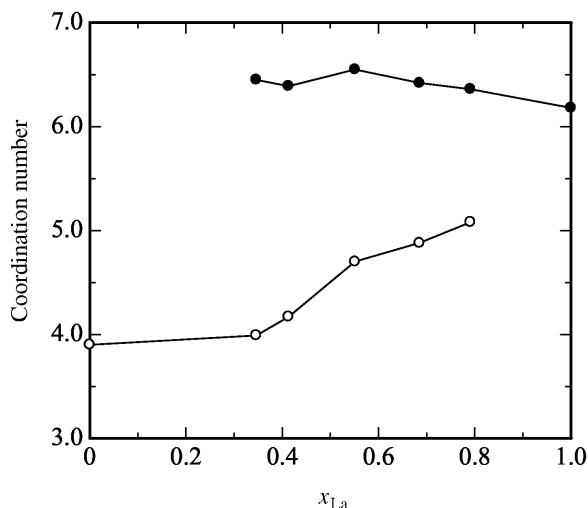
Fig. 2. The running coordination numbers in molten (La$_{1/3}$, K)Cl at 1173 K; white circles, K-Cl; black circles, La-Cl.

Fig. 3. Evolution for molten (La$_{1/3}$, K)Cl of the average distance of marked cations to Cl$^-$; solid lines, La^{3+}; broken lines, K$^+$; (a) $x_{La} = 0.346$; (b) $x_{La} = 0.792$.

for the peak heights, g_{La-Cl} is stronger in the binary mixtures than in pure LaCl$_3$ and is decreasing with increasing mole fraction of lanthanum. The location of the K$^+$ ion was discussed from the La-K, K-Cl and K-K correlations. In mutual comparison with the first peak positions in the $g_{ij}(r)$'s of three distinct correlations, the K-Cl correlation possessed a sharp peak at $r = 0.264 - 0.270$ nm, independent of LaCl$_3$ concentration. It is natural that $n_{La-K}(r)$ decreased with increasing LaCl$_3$ concentration, and most interesting was that the mode of the first peak in $g_{La-K}(r)$ was situated around $r_{La-K} = 0.508$ nm at $x_{La} = 0.346$. In contrast, the corresponding value was reduced to 0.492 nm at $x_{La} = 0.792$. This result was qualitatively thought to show that the linkage of the [LaCl$_6$]$^{3-}$ units was broken with adding of KCl, and thus the K$^+$ ions resulted in entering in the gap grown between the new born octahedra. This behavior is consistent with the experimental results for the electrical properties [24] and similar to that of (Dy$_{1/3}$, K)Cl [11] and (Nd$_{1/3}$, K)Cl [12].

The separating motion of cation-anion pairs could be expressed in terms of the self-exchange velocity (SEV), which was simulated by molecular dynamics methods. The evolution of the average distance of marked La^{3+} and K$^+$ ions from a Cl$^-$ ion for three compositions is shown in Figure 3. The SEV, v, which was correlated with internal mobility [25], is defined as
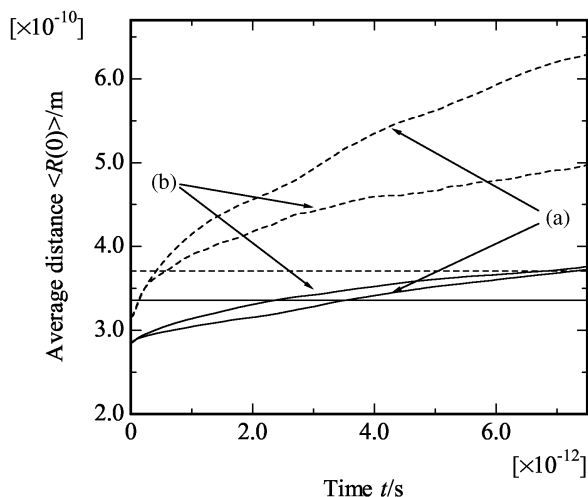
$$v = \frac{(R_2 - \langle R(0) \rangle)}{\tau}, \tag{3}$$

where R_2 is the distance at which $g(r)$ between cation and anion reaches unity after the first peak, R_1, and $\langle R(0) \rangle$ is the average distance of cations located within R_2 from a reference anion at $t = 0$. $t = \tau$ is the average time in which the mean distance of such particles becomes R_2. Thus, the SEV is the velocity of the separating motion of two neighboring unlike ions and could be estimated with good accuracy from relatively short MD simulation steps, because each anion has several neighboring cations. For the present system the SEV was calculated from 150 origins for molten binary mixtures. The solid and broken lines exhibited in Fig. 3 indicate R_2 for La and K, respectively.

The obtained SEV's for La and K are summarized in Table 2, which shows that the SEV of La is smaller than that of K at all compositions. The strong correlation between the internal mobilities and the SEV's for some alkali chlorides has already been reported [25]. The relationship between the internal cation mobility, b, and the SEV in (La$_{1/3}$, K)Cl and (Dy$_{1/3}$, K)Cl is shown in Figure 4. These experimentally obtained b values of K$^+$ and La^{3+} are calculated from (4a) and (4b), using the ε values available, the electrical conductivities κ and equivalent volumes V_e of the mixtures:

$$b_K = (\kappa V_e/F)(1 + \varepsilon x_{La}), \tag{4a}$$

$$b_{La} = (\kappa V_e/F)(1 - \varepsilon x_K), \tag{4b}$$

where x is the equivalent fraction. The value of b_{La} increases with x_{La}. The Cl$^-$ ions associate to the La^{3+}

x_{La}	κ_{exp} [5] (S m^{-1})	κ_{cal} (S m^{-1})	$b_{La,exp}$ [5] (10^{-8} m^2 V^{-1} s^{-1})	$b_{K,exp}$ [5] (10^{-8} m^2 V^{-1} s^{-1})	SEV$_{La}$ (m s^{-1})	SEV$_K$ (m s^{-1})	$D_{La,cal}$ (10^{-9} m^2 s^{-1})	$D_{K,cal}$ (10^{-9} m^2 s^{-1})
0	212.0	187.2	—	10.30	—	—	—	3.62
0.346	112.2	95.2	0.67	7.19	14.31	62.15	0.75	3.23
0.413	107.5	92.4	1.87	6.52	15.58	58.32	0.92	2.74
0.551	111.2	88.2	2.31	7.06	17.86	54.62	1.18	2.23
0.685	121.9	84.4	3.11	7.38	19.54	52.75	1.25	2.04
0.792	121.8	82.6	3.71	5.30	21.58	44.28	1.44	1.81
1.000	113.0	81.6	2.77	—	—	—	1.65	—

Table 2. Main experimental results and characteristic parameters obtained from MD simulation in molten LaCl$_3$-KCl at 1123 K.
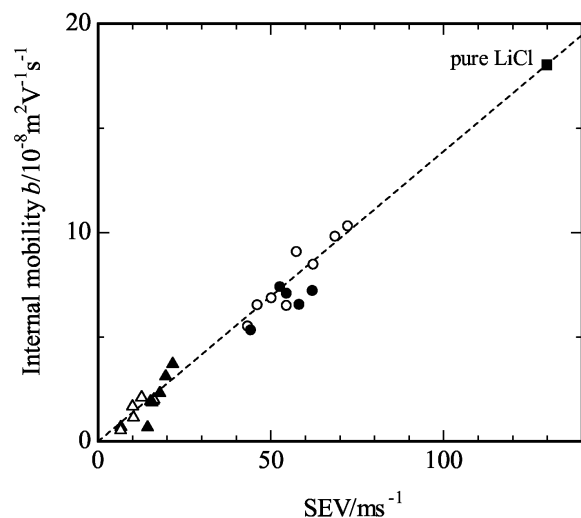

Fig. 4. Relation between the internal cation mobility and self-exchange velocity (SEV) in molten (La$_{1/3}$, K)Cl at 1123 K and (Dy$_{1/3}$, K)Cl [11] at 1093 K; La^{3+}, black triangles; K$^+$ in (La$_{1/3}$, K)Cl, black circles; Dy^{3+}, white triangles; K$^+$ in (Dy$_{1/3}$, K)Cl, white circles; Li$^+$ in pure LiCl [26], black square.

Fig. 5. Relation between the self-diffusion coefficients and the mole fractions of La and κ in molten (La$_{1/3}$, K)Cl at 1123 K; La^{3+}, black circles; K$^+$, white circles.

ions and form the complexes of [LaCl$_6$]$^{3-}$ such as [DyCl$_6$]$^{3-}$ in the (Dy$_{1/3}$, K)Cl [11]. The anion species of [LaCl$_6$]$^{3-}$ in high composition of La^{3+} ion are less stable than those in low composition of La^{3+} ion due to a shortage of Cl$^-$ ion. Then the values of b_{La} might be almost zero at the low composition of La^{3+} ion owing to the stabilization of [LaCl$_6$]$^{3-}$. On the contrary, the value of b_K decreases with increasing concentration of La^{3+}. This would be due to the tranquilization effect [26], i.e., Cl$^-$ ions in the complexes of [LaCl$_6$]$^{3-}$ approache slowly the K$^+$ ions because [LaCl$_6$]$^{3-}$ is very massive. Therefore, the separating motion of the K$^+$ ion from the neighboring Cl$^-$ ion is slow, and b_K decreases. The decrease of b_{La} and SEV$_{La}$ with decreasing concentration of La^{3+} would be caused mainly by the charge-asymmetry stated below rather than by the increase in the equivalent volume. Owing to the charge asymmetry of the coordinat-
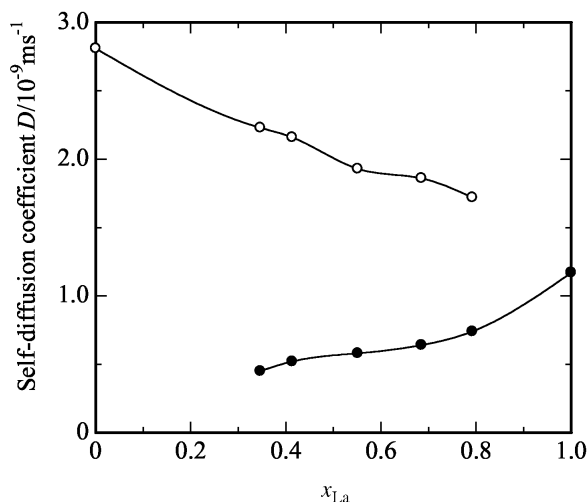
ing cations about the Cl$^-$ ions and consequently associates such as [LaCl$_6$]$^{3-}$ will have a longer life time. The formation of such species as [LaCl$_6$]$^{3-}$ with increasing x_K could be explained based on the Coulomb interaction. Consequently, it seems that there is an approximately linear relation between two entities and the ionic behavior is reproduced by SEVs obtained from the simulation.

At the time t the square displacement of a particle i is $r_i^2 = |r_i(t) - r_i(0)|^2$. The mean square displacement of N particles is thus defined by

$$r^2(t) = \frac{1}{N}\left\langle \sum_{i=1}^{N} |r_i(t) - r_1(0)|^2 \right\rangle. \tag{5}$$

The self-diffusion coefficients of La and K in molten LaCl$_3$-KCl are evaluated as

$$D = \lim_{t \to \infty} \frac{1}{6} r^2(t). \tag{6}$$

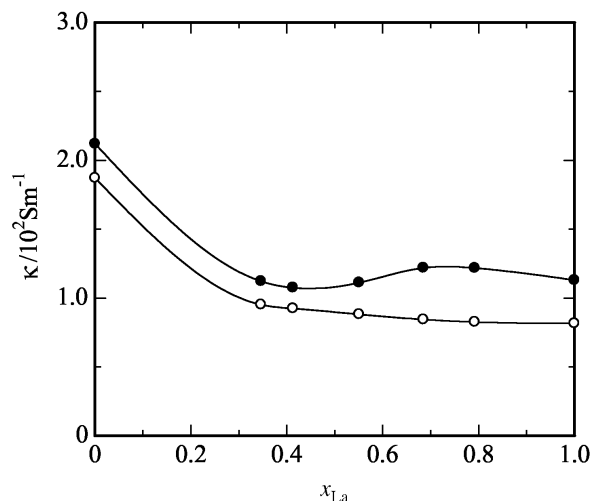The calculated and experimental results are represented in Fig. 5 and tabulated in Table 2, which

Fig. 6. Relation between the electrical conductivity and the mole fraction of La in molten (La$_{1/3}$, K)Cl at 1123 K; experimental results in (La$_{1/3}$, K)Cl [5], black circles; MD simulation in (La$_{1/3}$, K)Cl, white circles.

shows that the self-diffusion coefficients of La^{3+} increase with increasing concentration of La and the self-diffusion coefficients of K$^+$ decrease with decreasing concentration of K. This is consistent with observations on our calculated self-exchange velocities and the experimental internal cation mobilities. The tendency of the self-diffusion coefficient of La^{3+} and K$^+$ is consistent with the results for Dy^{3+} and K$^+$ in (Dy$_{1/3}$, K)Cl melts [11].

The electrical conductivity is estimated from the response to an applied external field. The strength of the external field is a magnitude such that the current is a linear function of the field. The increase of the internal energy caused by the external field is truncated by the Nose method, which makes it possible to keep the temperature constant. The definition of the current velocity is written as

$$j = |j_+| + |j_-|, \quad j_\pm = \sum_{i=1}^{N_\pm} z_i v_i. \tag{7}$$

The relation between the current velocity and the electric field is indicated as

$$\sigma = \frac{ej}{VE}, \tag{8}$$

where e means the elementary electric charge, V is the volume of the system, and E the magnitude of the external field. The electrical conductivity and the partial electrical conductivity are estimated from (8). The

electrical conductivity calculated from the MD simulation by comparison with the experimental results is expressed in Figure 6. The tendency could be reproduced by MD simulation, *i.e.*, the electrical conductivity is decreasing with increasing the concentration of La, although the values calculated from the MD simulation are smaller than the experimental results. The quantitative discrepancy for some transport properties between the experimental and simulated values remains unexplained.

From the consideration of the thermodynamic properties of LaCl$_3$-KCl [27], the following findings were demonstrated. The stability of the octahedron in molten LaCl$_3$ changes with adding KCl, though the fundamental structure around the La ion does not change. In the single salt, the number of Cl$^-$ ions would not be sufficient to build a network of octahedrally-coordinated structure. On the other hand, the octahedron becomes stable by supplying Cl$^-$ ions from the alkali chloride. The octahedron [LaCl$_6$]$^{3-}$ is more strongly stabilized by the larger K$^+$ ion compared with the smaller Na$^+$ ion. This stability of the octahedron and the medium range structural order are strongly affected by the ionic size. Better precision could be obtained by considering the polarization effect in further simulations.

4. Conclusion

This electromigration method could be applicable for the effective separation of the rare earth ions from the alkali ions, because b_K and v_K are much greater than b_{La} and v_{La} in the whole concentration range. As the concentration of La^{3+} increases, b_K, v_K and D_K considerably decrease. This decrease is caused by the tranquilization effect of La^{3+}, which strongly interacts with common Cl$^-$ ions. As the composition of K$^+$ increases, b_{La}, v_{La} and D_{La} gradually decrease and become very small at concentrations rich in KCl. This decrease could lead to a promoted association of species containing La^{3+} and generation of the long-lived species [LaCl$_6$]$^{3-}$. The linkage of the distorted octahedral network structure is broken with the enhancement of alkali chloride. Finally, the transport properties such as the internal mobility, the self-diffusion coefficient and the electrical conductivity in molten rare earth-alkalichloride mixtures by MD simulation were estimated and consistent with the experimental results.

[1] M. Matsumiya and R. Takagi, Z. Naturforsch. **55a**, 673 (2000).

[2] M. Matsumiya, R. Takagi, and R. Fujita, J. Nucl. Sci. Technol. **34**, 310 (1997).

[3] M. Matsumiya, H. Matsuura, R. Takagi, and R. Fujita, J. Electrochem. Soc. **147**, 11 (2000).

[4] M. Matsumiya, H. Matsuura, R. Takagi, and R. Fujita, J. Alloys Compd. **306**, 87 (2000).

[5] M. Zablocka-Malicka and W. Szczepaniak, J. Mol. Liq. **83**, 57 (1999).

[6] H. Matsuura, I. Okada, R. Takagi, and Y. Iwadate, Z. Naturforsch. **53a**, 45 (1998).

[7] R. Ohashi, M. Matsumiya, H. Matsuura, and R. Takagi, Electrochemistry **67**, 550 (1999).

[8] M. Matsumiya and R. Takagi, Z. Naturforsch. **55a**, 856 (2000).

[9] M. Matsumiya and R. Takagi, Z. Naturforsch. **56a**, 279 (2001).

[10] M. Matsumiya, W. Shin, N. Izu, and N. Murayama, J. Electroanal. Chem. **528**, 103 (2002).

[11] M. Matsumiya and R. Takagi, Z. Naturforsch. **56a**, 273 (2001).

[12] M. Matsumiya and R. Takagi, Z. Naturforsch. **56a**, 466 (2001).

[13] S. Nose, Mol. Phys. **52**, 255 (1984).

[14] P. P. Ewald, Ann. Phys. **64**, 253 (1921).

[15] M. P. Tosi and F. G. Fumi, J. Phys. Chem. Solids **25**, 45 (1964).

[16] Y. Iwadate, J. Mochinaga, and K. Kawamura, J. Phys. Chem. **85**, 3708 (1981).

[17] G. J. Janz, J. Phys. Chem. Ref. Data **17**, 1 (1988).

[18] B. Larsen, T. Forland, and K. Singer, Mol. Phys. **26**, 1521 (1973).

[19] L. V. Woodcock, Chem. Phys. Lett. **10**, 257 (1971).

[20] J. P. Hansen and I. R. McDonald, Theory of Simple Liquids, Academic Press, London 1986.

[21] G. N. Papatheodorou, J. Chem. Phys. **66**, 2893 (1977).

[22] G. M. Photiadis, B. Borrensen, and G. N. Papatheodorou, J. Chem. Soc., Faraday Trans. **94**, 2605 (1998).

[23] Y. Okamoto, H. Shiwaku, T. Yaita, H. Narita, and H. Tanida, J. Mol. Struct. **64**, 71 (2002).

[24] I. Okada, R. Takagi, and K. Kawamura, Z. Naturforsch. **35a**, 493 (1980).

[25] T. Koura, H. Matsuura, and I. Okada, J. Mol. Liq. **73–74**, 195 (1997).

[26] J. Habasaki, C.-C. Yang, and I. Okada, Z. Naturforsch. **42a**, 695 (1987).

[27] G. N. Papatheodorou and T. Ostvold, J. Phys. Chem. **78**, 181 (1974).